Velocity Estimation Error Reduction in Stenosis Areas Using a Correlation Correction Method

Luzhen Nie, Sevan Harput, David M. J. Cowell and Steven Freear
Ultrasonics and Instrumentation Group, School of Electronic and Electrical Engineering, University of Leeds, UK.
E-mail: elln@leeds.ac.uk and s.freear@leeds.ac.uk

***Abstract*—The advent of ultrafast ultrasound imaging proved beneficial for capturing transient flow patterns which was never readily achievable before. Velocity estimation methods based on 2D block-matching outperform Doppler based methods by offering higher frame rate with the cost of increased uncertainty in presence of out-of-plane motion as a result of turbulent flow.**

Local median filtering can partially address the estimation error reduction in stenosis areas at the risk of higher inaccuracy, since neighboring values may be also outliers. In this study, a correlation correction method is proposed, where the out-of-plane motion is eliminated by means of multiplying correlation maps from a same area but in two adjacent pairs of RF images.

Experimental investigations were performed on a wall-less flow phantom, and proposed method achieved an error reduction of 66% in turbulent flow regions.

I. Introduction

Ultrasonic imaging underpins quantifications of blood flow for many cardiovascular diseases which manifest strong flow abnormalities. Conventional color flow Doppler prevails in real-time imaging but confined by fundamental limitations such as angle-dependence, aliasing [1] and low frame rate. Angle dependence and aliasing can be partially approached by angle correction and shifting the Doppler frequency baseline respectively [2], but the following-up monitoring of disease progression is hampered due to large inter-operator velocity fluctuations.

More intuitive and accurate angle-independent 2D diagnosis modalities have been suggested varying from vector Doppler [3], transverse oscillation [4] to directional beamforming [5], speckle tracking [6] and echo particle image velocimetry [7]. Ultrafast imaging especially plane wave imaging (PWI) [8], in which thousands of frames per second can be achievable by sacrificing the transmit focusing where the resolution is recovered later by receive beamforming techniques, has attracted renewed attention in color Doppler imaging [9], and particularly 2D vector flow mapping techniques [10]–[12].

Speckle tracking based methods enable aliasing-free flow imaging with higher frame rate which potentially provide good insight into diagnosing diseases showing transient abnormal flow patterns. But it's still very challenging to portray turbulent flow over narrowed blood vessels during 2D blood flow measurements as a result of strong out-of-plane motion, and block-matching based techniques are prone to inaccurate results due to speckle pattern decorrelation between adjacent frames.

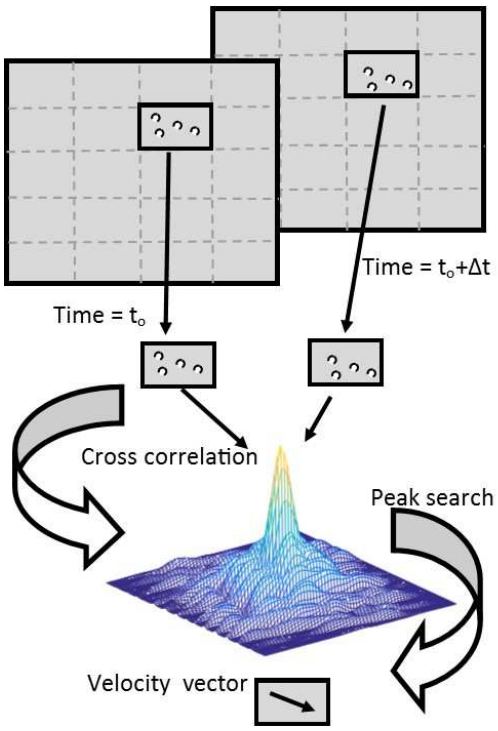

Fig. 1. Basic principle of 2D block-matching methods based on frame-to-frame cross-correlation.

Out-of-plane motion artefacts imposed by turbulent flow in block-matching based methods have been seldom addressed. This manuscript investigates the feasibility of adopting a correlation correction method in conjunction with ultrafast PWI to reduce velocity estimation outliers in stenotic regions which permits more accurate velocity estimations.

II. Methodology

A. Contrast Enhanced PWI

Acquisition of thousands of frames real time by using PWI could potentially improve the vascular disease diagnosis and give great insight into progression monitoring of vascular stenosis. The high frame rate comes with a cost of lower penetration depth and poor signal to noise ratio (SNR) due to the lack of transmitting focus in ultrafast imaging. However, when contrast agents are introduced into the blood stream the image SNR becomes high enough to detect microbubbles [12].

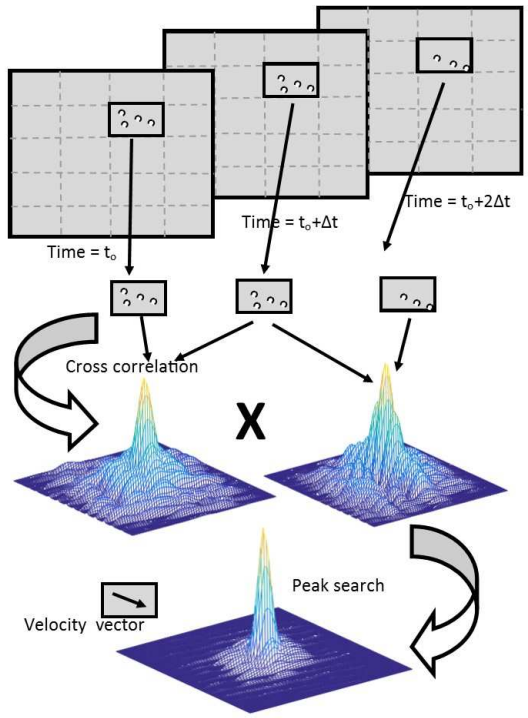

Fig. 2. Demonstration of correlation-correction method.

B. Signal Processing

1) Correlation Based Velocity Estimation: The principle of velocity estimation basically relies on displacement computation with two same-size interrogation windows in adjacent frames as depicted in Figure 1, with the assumption that particles follow the true stream and PWI enables small displacements in successive frames. Given the highest correlation peak position and the time interval between neighboring frames, the averaged velocity is obtained. For the sake of computational efficiency, direct cross correlation given by (1) or (2) can be replaced by FFT based cross correlation ((3), (4)) in frequency domain so as to display hundreds of vectors in a reasonable time-scale.

$$\Phi(m,n) = \sum_i \sum_j f(i,j)g(i+m,j+n) \tag{1}$$

$$\Phi(m,n) = \frac{\sum_i \sum_j [f(i,j) - \overline{f}][g(i+m,j+n) - \overline{g}]}{\sqrt{\sum_i \sum_j [f(i,j) - \overline{f}]^2 [g(i+m,j+n) - \overline{g}]^2}} \tag{2}$$

Where Φ denotes the cross correlation coefficient map, f and g two kernels in two frames, m and n the integer pixel offset (both zero in this study), $\overline{f}$ and $\overline{g}$ the averaged distribution value.

$$\Phi(m,n) = f^{\star}(-m,-n) * g \tag{3}$$

Based on the convolution theorem, (3) can be deduced to:

$$\Phi(m,n) = \text{iFFT}(\text{F}^{\star}(f)\text{F}(g)) \tag{4}$$

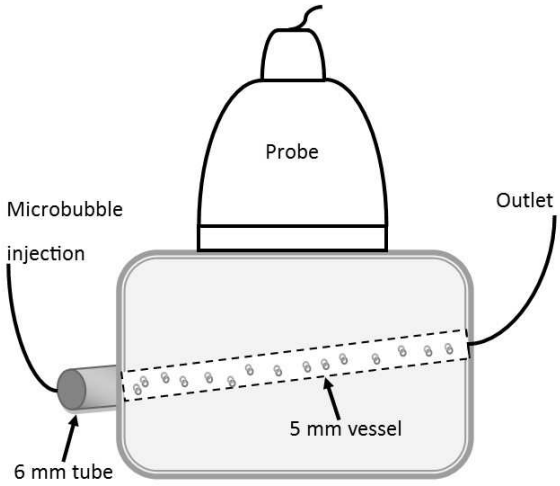

Fig. 3. Experimental setup: a wall-less tissue mimicking flow phantom with varying vessel diameters.

Where $\star$ indicates complex conjugate, $*$ the convolution, and F denotes the Fourier transform, iFFT the inverse Fourier transform.

2) Sub-pixel Peak Finding in Cross-Correlation Maps: Integer pixel displacements are not guaranteed, an Gaussian interpolation method is introduced into post processing as given by [13] and illustrated as (5) and (6).

$$\Delta i = \frac{\ln[\Phi(i,j-1)] - \ln[\Phi(i,j+1)]}{2\ln[\Phi(i,j-1)] - 4\ln[\Phi(i,j)] + 2\ln[\Phi(i,j+1)]} \tag{5}$$

$$\Delta j = \frac{\ln[\Phi(i-1,j)] - \ln[\Phi(i+1,j)]}{2\ln[\Phi(i-1,j)] - 4\ln[\Phi(i,j)] + 2\ln[\Phi(i+1,j)]} \tag{6}$$

Where i and j are integer pixel coordinates at which the maximum cross correlation coefficient is reached, Δi and Δj, the sub-pixel estimations.

3) Correlation Correction: Regarding merits of PWI, in-plane flow patterns within small kernels during several plane wave insonifications can be assumed relatively constant compared with out-of-plane motion. The elimination of this motion artefact is achieved by multiplying correlation maps from a same area but in two neighbouring pairs of RF images, as only the in-plane motion both in each of the map can be enhanced. Reduced mainlobe width and sidelobe levels in 2D correlation maps are also beneficial for sub-pixel peak finding (Figure 2).

C. Materials and Experiments

A wall-less gel tissue mimicking flow phantom was built with varying vessel diameters to generate turbulent flow at the vessel inlet (Figure 3). Diluted SonoVue® microbubble solution with a clinically relevant concentration was driven by a syringe pump (*Aladdin AL-1000, World Precision Instruments*) with a constant volume rate of 24 ml/minute.

TABLE I
PARAMETERS OF TRANSDUCER SETUP AND DATA ACQUISITION

Parameter	Value
Number of elements	128
Pitch	0.3048 mm
Center Frequency (f_c)	5 MHz
Bandwidth (B)	3-8 MHz
Excitation signal	Negative pulse
UARP II channels	128
Sampling Frequency (f_s)	80 MHz
Imaging depth	45 mm
Receive apodization	Hann window

A L3-8/40EP medical transducer (*Prosonic.co, Ltd, Korea*) was connected to the in-house built ultrasound array research platform II (UARP II) [14], [15] which is capable of providing arbitrary excitation schemes, and ultrafast PWI at 500 Hz was acquired by firing all the 128 elements of the linear transducer array with negative excitation pulse controlled by the Leeds UARP II.

The time gain compensation together with the frequency based attenuation compensation were carried out. RF raw data with imaging depth up to 45 mm was sampled with 80 MHz sampling frequency and saved into local memory of a desktop computer followed by delay-and-sum beamformation [16]. Also from the perspective of clinical practice, hemodynamic information was superimposed on anatomic B-mode images which were presented with 40 dB dynamic range. Details of transducer setup and acquisition parameters are listed in Table I.

D. Experimental Results

A binary mask was adopted to define the region of interest, and totally a batch of one hundred RF frames after delay-and-sum beamformer underwent velocity estimation and evaluation. With the flow phantom geometry and volume rate, the Reynold number was estimated to be 105 which is smaller than 1817 for turbulence formation according to the formula (7) [12]. The flow inside the vessel ought to feature a turbulent pattern at the inlet while keeps an constant manner later on (Figure 4 and Figure 5). Entrance length for laminar flow is calculated to be around 21 mm following formula (8) demonstrated in [12].

$$Re = vdp/u \tag{7}$$

$$L = 0.04dRe \tag{8}$$

Where *Re* denotes the Reynolds number, *v* the mean velocity in the vessel, *d* the vessel diameter, *p* the solution density, *u* refers to the viscosity and L being the inlet length for laminar flow generation.

A correlation signal-to-noise ratio (SNR) threshold of 0.7 was used to separate estimation anomalies (green arrows in Figure 5) from valid ones. Those vectors derived from correlation maps with lower correlation SNR than the threshold were marked as outliers. The proposed method reduced inaccurate vectors with a mean percentage of 66% as can be clearly seen in Figure 5 (b).

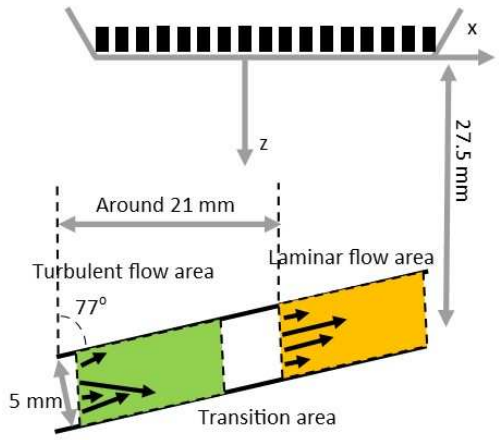

Fig. 4. Schematic diagram of flow patterns in the phantom.

Estimation evaluation along three lines within laminar flow area described in Figure 4 was explained in Figure 6 with emphasis on fluctuations before and after correlation correction. Mean bias is nearly same at all locations but the correlation correction method prevails in smaller deviation in some cases.

III. DISCUSSION AND CONCLUSIONS

Few methods have been suggested to reduce out-of-plane motion artefacts in 2D ultrasonic velocity mapping. Post-processing algorithms, such as local median filtering, fail to reduce estimation errors in stenotic regions since vectors in adjacent sub-windows may be also outliers due to turbulent flow.

While the lack of ground truth in turbulent flow is still an obstacle for accurate evaluation of the proposed method, and incapability of portraying 3D information indicates a second drawback. The proposed correlation correction method has proven beneficial for error reduction in turbulent flow area with a percentage of 66% in terms of a SNR threshold in correlation maps and additional benefits of smaller fluctuations for laminar flow are also recognized.

The introduction of microbubbles further makes it possible to enhance contrast to noise ratio and enable more accurate estimations by means of contrast pulse sequences [17] or subharmonic imaging [18].

REFERENCES

[1] J. A. Jensen and P. Munk, "A new method for estimation of velocity vectors," *IEEE Transactions on Ultrasonics, Ferroelectrics, and Frequency Control*, vol. 45, no. 3, pp. 837–851, May 1998.

[2] R. W. Gill, "Measurement of blood flow by ultrasound: accuracy and sources of error," *Ultrasound in Medicine & Biology*, vol. 11, no. 4, pp. 625–641, 1985.

[3] B. Dunmire, K. Beach, K. Labs, M. Plett, and D. Strandness, "Cross-beam vector doppler ultrasound for angle-independent velocity measurements," *Ultrasound in Medicine & Biology*, vol. 26, no. 8, pp. 1213–1235, 2000.

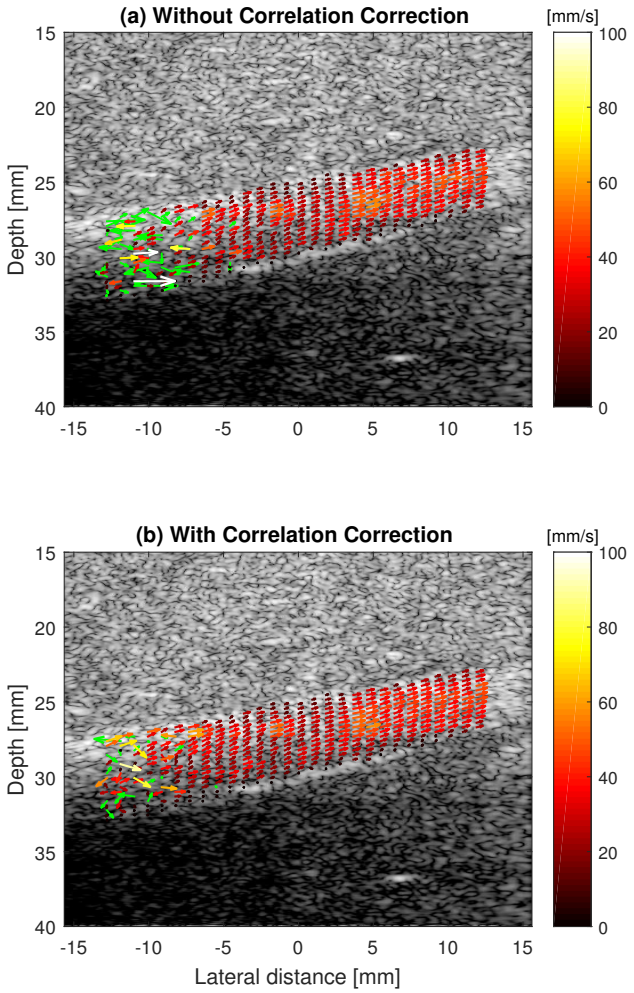

Fig. 5. A pair of experimental examples: velocity estimations (a) without correlation correction and (b) after correlation correction. Error arrows are highlighted in green.

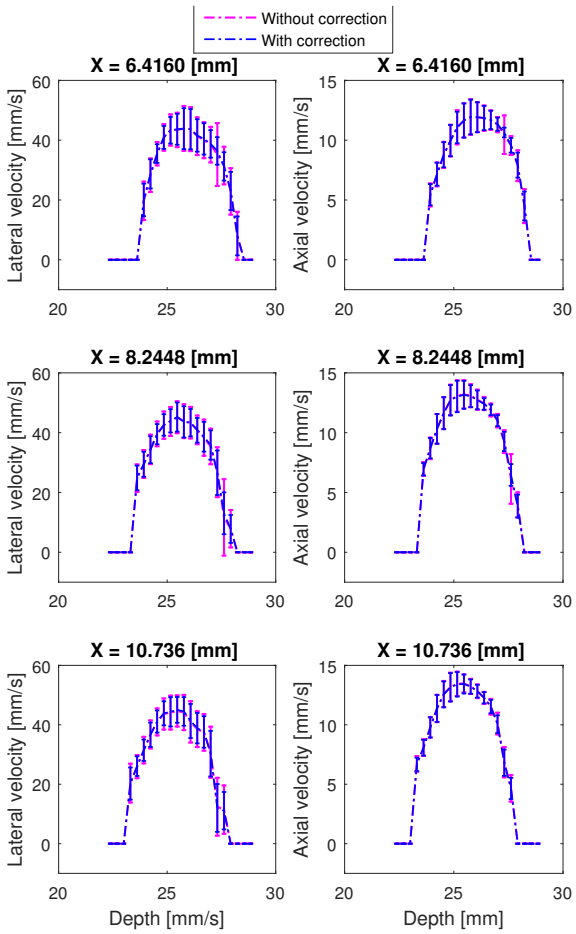

Fig. 6. Lateral and axial velocity estimations with and without correlation correction along three lines located at lateral distance 6.4160 mm, 8.2488 mm and 10.736 mm in the constant flow field detailed in Figure 4.

[4] J. Udesen and J. A. Jensen, "Investigation of transverse oscillation method," *IEEE Transactions on Ultrasonics, Ferroelectrics, and Frequency Control*, vol. 53, no. 5, pp. 959–971, 2006.

[5] A. Jensen and S. I. Nikolov, "Directional synthetic aperture flow imaging," *IEEE Transactions on Ultrasonics, Ferroelectrics, and Frequency Control*, vol. 51, no. 9, pp. 1107–1118, 2004.

[6] L. Bohs, B. Geiman, M. Anderson, S. Gebhart, and G. Trahey, "Speckle tracking for multi-dimensional flow estimation," *Ultrasonics*, vol. 38, no. 1, pp. 369–375, 2000.

[7] H. Kim, J. Hertzberg, and R. Shandas, "Development and validation of echo piv," *Experiments in Fluids*, vol. 36, no. 3, pp. 455–462, 2004.

[8] M. Tanter, J. Bercoff, L. Sandrin, and M. Fink, "Ultrafast compound imaging for 2-d motion vector estimation: application to transient elastography," *IEEE Transactions on Ultrasonics, Ferroelectrics, and Frequency Control*, vol. 49, no. 10, pp. 1363–1374, 2002.

[9] B. F. Osmanski, M. Pernot, G. Montaldo, and M. Tanter, "Imaging blood flow dynamics within fast moving tissue: Application to the myocardium," in *2011 IEEE International Ultrasonics Symposium*, Oct 2011, pp. 272–275.

[10] M. Lenge, A. Ramalli, P. Tortoli, C. Cachard, and H. Liebgott, "Plane-wave transverse oscillation for high-frame-rate 2-d vector flow imaging," *IEEE Transactions on Ultrasonics, Ferroelectrics, and Frequency Control*, vol. 62, no. 12, pp. 2126–2137, 2015.

[11] C. A. V. Hoyos, M. B. Stuart, K. L. Hansen, M. B. Nielsen, and J. A. Jensen, "Accurate angle estimator for high-frame-rate 2-d vector flow imaging," *IEEE Transactions on Ultrasonics, Ferroelectrics, and Frequency Control*, vol. 63, no. 6, pp. 842–853, 2016.

[12] C. H. Leow, E. Bazigou, R. J. Eckersley, C. Alfred, P. D. Weinberg, and M.-X. Tang, "Flow velocity mapping using contrast enhanced high-frame-rate plane wave ultrasound and image tracking: Methods and initial in vitro and in vivo evaluation," *Ultrasound in Medicine & Biology*, vol. 41, no. 11, pp. 2913–2925, 2015.

[13] L. Niu, J. Wang, M. Qian, and H. Zheng, "Sub-piexl methods for improving vector quality in echo piv flow, imaging technology," in *2009 Annual International Conference of the IEEE Engineering in Medicine and Biology Society*. IEEE, 2009, pp. 487–490.

[14] D. Cowell and S. Freear, "Quinary excitation method for pulse compression ultrasound measurements," *Ultrasonics*, vol. 48, no. 2, pp. 98–108, 2008.

[15] D. M. Cowell, P. R. Smith, and S. Freear, "Phase-inversion-based selective harmonic elimination (pi-she) in multi-level switched-mode tone- and frequency-modulated excitation," *IEEE Transactions on Ultrasonics, Ferroelectrics, and Frequency Control*, vol. 60, no. 6, pp. 1084–1097, 2013.

[16] G. Montaldo, M. Tanter, J. Bercoff, N. Benech, and M. Fink, "Coherent plane-wave compounding for very high frame rate ultrasonography and transient elastography," *IEEE Transactions on Ultrasonics, Ferroelectrics, and Frequency Control*, vol. 56, no. 3, pp. 489–506, 2009.

[17] P. Phillips, "Contrast pulse sequences (cps): imaging nonlinear microbubbles," in *Ultrasonics Symposium, 2001 IEEE*, vol. 2. IEEE, 2001, pp. 1739–1745.

[18] S. Harput, M. Arif, J. McLaughlan, D. M. Cowell, and S. Freear, "The effect of amplitude modulation on subharmonic imaging with chirp excitation," *IEEE Transactions on Ultrasonics, Ferroelectrics, and Frequency Control*, vol. 60, no. 12, pp. 2532–2544, 2013.